

Superconducting Qubit Storage and Entanglement with Nanomechanical Resonators

A. N. Cleland¹ and M. R. Geller²

¹*Department of Physics, University of California, Santa Barbara, California 93106, USA*

²*Department of Physics and Astronomy, University of Georgia, Athens, Georgia 30602-2451, USA*

(Received 14 September 2003; revised manuscript received 15 December 2003; published 10 August 2004)

We propose a quantum computing architecture based on the integration of nanomechanical resonators with Josephson-junction phase qubits. The resonators are GHz-frequency, dilatational disk resonators, which couple to the junctions through a piezoelectric interaction. The system is analogous to a collection of tunable few-level atoms (the Josephson junctions) coupled to one or more electromagnetic cavities (the resonators). Our architecture combines desirable features of solid-state and optical approaches and may make quantum computing possible in a scalable, solid-state environment.

DOI: 10.1103/PhysRevLett.93.070501

PACS numbers: 03.67.Pp, 03.67.Lx, 85.25.Cp, 85.85.+j

The lack of a scalable qubit architecture, with both a sufficiently long quantum-coherence lifetime and a controllable entanglement scheme, is the principal roadblock to building a large-scale quantum computer. Superconducting devices are natural qubit candidates because they exhibit robust, macroscopic quantum behavior [1]. Recently, there have been exciting demonstrations of long-lived Rabi oscillations in current-biased Josephson junctions [2,3], subsequently combined with a two-qubit capacitive coupling scheme [4]. There have also been beautiful demonstrations of Rabi oscillations, Ramsey fringes, and two-qubit quantum logic in Cooper-pair box geometries [5]. These accomplishments have generated tremendous interest in the potential for superconductor-based quantum computers. Coherence times up to 5 μ s have been reported in the current-biased devices [2], long enough to perform many logical operations.

Here we describe a flexible and scalable quantum-information-processing architecture in which GHz-frequency piezoelectric dilatational resonators couple two or more large-area, current-biased Josephson-junction (JJ) *phase* qubits. We present data already showing unprecedented performance at 4.2 K of a 1.8 GHz AlN resonator, which will serve as the coupling element. We also show theoretically that such resonators can act as high-fidelity quantum memory and bus elements and can be used to produce entangled junction states and mediate quantum logic. Other investigators have proposed the use of electromagnetic [6] or superconducting [7] resonators to couple JJs together. The use of mechanical resonators in quantum computing has not to our knowledge been considered previously, although an interesting method to create entangled states of a beam resonator and charge qubit has been proposed by Armour *et al.* [8]. Resonator-based qubit couplings allow for a variety of frequency-tuned interactions between two or more JJs connected to the same resonator. The use of on-chip mechanical resonators has the advantage that potentially much higher quality factors and smaller dimensions can be achieved simultaneously, enabling a truly scalable approach.

Our implementation uses large-area current-biased JJs, with capacitance C and critical current I_0 , as shown in Fig. 1. The largest relevant energy scale is the Josephson energy $E_J \equiv \hbar I_0/2e$, with the charging energy $E_c \equiv (2e)^2/2C$ much smaller than E_J . The dynamics of the JJ phase difference δ is that of a particle of “mass” $M = \hbar^2 C/4e^2$ moving in an effective potential $U(\delta) \equiv -E_J(\cos\delta + s\delta)$, where $s \equiv I_b/I_0$ is the dimensionless bias current [9]. When $0 < s < 1$, $U(\delta)$ has metastable minima, separated from the continuum by a barrier of height ΔU , also shown in Fig. 1. The small-oscillation plasma frequency is $\omega_p = \omega_{p0}(1 - s^2)^{1/4}$, with $\omega_{p0} = \sqrt{2E_J E_c}/\hbar$. The Hamiltonian for an isolated JJ in the $R \rightarrow \infty$ limit is $H_J = -E_c d^2/d\delta^2 + U(\delta)$, with quasi-bound states in the minima with energies ϵ_m . The lowest energy quasibound states $|0\rangle$ and $|1\rangle$ define a *phase* qubit, with $\Delta E \equiv \epsilon_1 - \epsilon_0$ the level spacing. We focus here on a single resonator coupled to one and two JJs; extensions to larger systems will be addressed in future work. The basic two-junction circuit is shown in Fig. 2. The disk-shaped element is the nanomechanical resonator, consisting of a piezoelectric crystal sandwiched between split metal electrodes, and the JJs are the crossed boxes.

The nanomechanical resonator is designed to have a fundamental thickness-resonance frequency $\omega_0/2\pi$ of a few GHz, and a high quality factor $Q \equiv \omega_0\tau$, where τ is

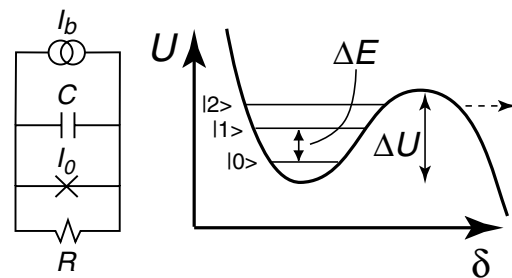


FIG. 1. Left: equivalent-circuit model for a current-biased JJ. A capacitance C and resistance R in parallel with an ideal Josephson element with critical current I_0 , all sharing a bias current I_b . Right: potential in the cubic $s \rightarrow 1^-$ limit.

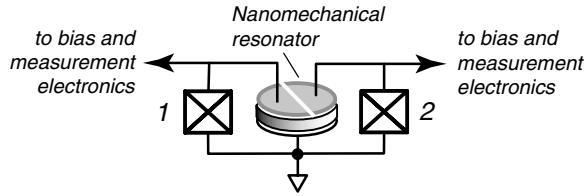


FIG. 2. Two phase qubits coupled to a piezoelectric resonator.

the energy damping time. Piezoelectric dilatational resonators with frequencies in this range, and with room-temperature quality factors around 10^3 , have been fabricated from sputtered AlN [10]. In Fig. 3 we present rf network measurements down to 4.2 K for a similar piezoelectric 1.8 GHz resonator, held by high acoustic impedance supports. The observed low-temperature Q of 3500 corresponds to an energy lifetime τ of more than 300 ns, already sufficient for the operations described below. This is to be contrasted with the current state-of-the-art 1 GHz SiC doubly clamped resonator demonstrated previously [11], which has a Q nearly an order of magnitude smaller at the same temperature. The unprecedented performance of our resonator is a consequence of the use of AlN, which is a high Q material [12], and the use of the dilatational vibrational mode. Upon cooling to 20 mK, the 1.8 GHz dilatational mode will be in the *quantum* regime, with a probability of thermally occupying the first excited (one phonon) state of about 10^{-2} . Using dilatational-phonon creation and annihilation operators, the resonator Hamiltonian is $H_{\text{res}} = \hbar\omega_0 a^\dagger a$.

An elastic strain in the resonator shown in Fig. 2 produces, through the piezoelectric effect, a charge q on the capacitor enclosing it, corresponding to a current \dot{q} . A model for a disk resonator of radius R and thickness b leads to $q = C_{\text{res}}(V - e_{33}bU_{zz}/\epsilon_{33})$, where $C_{\text{res}} = \epsilon_{33}\pi R^2/b$ is the resonator capacitance, V is the voltage across it, e_{33} and ϵ_{33} are the relevant elements of the piezoelectric modulus and dielectric tensors (the z direction perpendicular to the disk), and U_{zz} is the spatially averaged strain. Strain induces an electric field $E_z = e_{33}U_{zz}/\epsilon_{33}$ in the piezoelectric, and a charge of

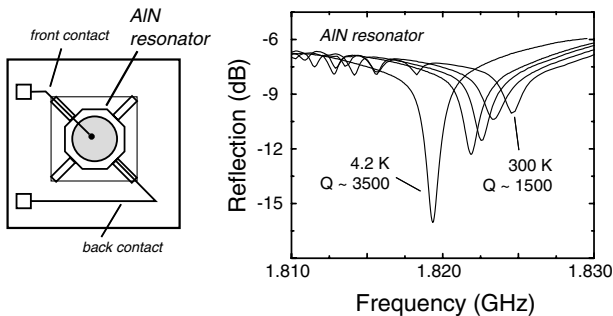


FIG. 3. Resonances measured in a 1.8 GHz AlN piezoelectric dilatational disk resonator, shown schematically on the left, from 300 down to 4.2 K. The resonance at 4.2 K has a quality factor of about 3500.

magnitude $\tilde{C}_{\text{res}}E_z b$ on the electrodes, where $\tilde{C}_{\text{res}} \equiv C_{\text{res}}/(1 - \gamma - \gamma^2)$ is a piezoelectrically enhanced capacitance ($\gamma \equiv e_{33}^2/\epsilon_{33}c_{33}$ is the piezoelectric coupling efficiency, and c_{33} the elastic stiffness). The resonator adds the capacitance \tilde{C}_{res} in parallel with the JJ capacitance, reducing the charging energy E_c to $2e^2/(C + \tilde{C}_{\text{res}})$.

Quantizing the vibrational modes of the resonator in the presence of the appropriate mechanical and electrodynamic boundary conditions leads to a Hamiltonian for a single JJ coupled to a resonator given by $H = H_J + H_{\text{res}} + \delta H$, where $\delta H = -ig(a - a^\dagger)\delta$, and

$$g \equiv \frac{\hbar^{3/2}e_{33}\tilde{C}_{\text{res}}\sqrt{\omega_0}}{e\epsilon_{33}\sqrt{\rho}\pi R^2 b} \quad (1)$$

is a real-valued coupling constant with dimensions of energy. For a JJ connected to one-half of a split-gate resonator, the relevant interaction strength is $g/2$. Here ρ is the mass density of the resonator material. The eigenstates of $H_J + H_{\text{res}}$ are $|mn\rangle \equiv |m\rangle_J \otimes |n\rangle_{\text{res}}$, with energies $E_{mn} = \epsilon_m + \hbar\omega_0 n$ (n is the resonator phonon occupation number), and an arbitrary state (for fixed bias) can be expanded as $|\psi(t)\rangle = \sum_{mn} c_{mn}(t)e^{-iE_{mn}t/\hbar}|mn\rangle$. The probability amplitudes c_{mn} are determined by

$$i\hbar\dot{c}_{mn} = \sum_{m'n'} \langle mn|\delta H|m'n'\rangle e^{i(E_{mn} - E_{m'n'})t/\hbar} c_{m'n'}. \quad (2)$$

A system of JJs and resonators is evidently similar to a collection of tunable few-level atoms (the junctions) in one or more electromagnetic cavities (the resonators). Here the “photons” are really resonator phonons, which interact with the “atoms” via the piezoelectric effect. However, here we can individually tune the level spacing of the atoms by varying bias currents and control the electromagnetic interaction strength by engineering the dimensions of the resonator [13]. We now describe elementary quantum-information-processing operations that should be possible with this rich architecture. We show that the quantum state of a JJ can be passed to the resonator and stored there and later passed back to the original JJ or to a different JJ. The resonator can also produce controlled entangled states of two JJs and can mediate quantum logic. These operations are performed by tuning the level spacing ΔE into resonance with $\hbar\omega_0$, thereby generating electromechanical Rabi oscillations.

We first show theoretically that we can pass a qubit state from a JJ to the resonator and store it there, using the adiabatic approximation combined with the rotating-wave approximation (RWA) of quantum optics [14]. The RWA is valid when the detuning $\hbar\omega_d \equiv \hbar\omega_0 - \Delta E$ satisfies $|\hbar\omega_d| \ll \hbar\omega_0/Q$ and $g \ll \Delta E$. We assume that s changes slowly on the time scale $\hbar/\Delta E$ and work at zero temperature. In the RWA, neglecting population and phase relaxation, we obtain from (2) the equations of motion

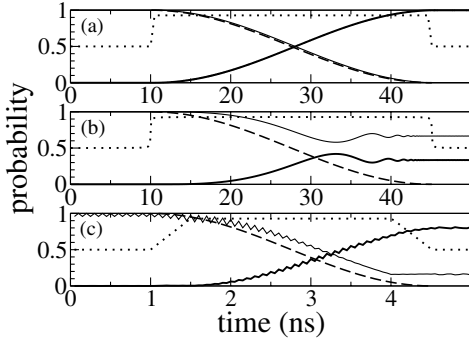


FIG. 4. Qubit storage in nanomechanical resonator. (a) Thin descending and thick ascending solid curves are $|c_{10}|^2$ and $|c_{01}|^2$, respectively. The dotted curve is s , which has a trapezoidal shape. The dashed curve is the RWA prediction for $|c_{10}|^2$. (b) Qubit storage with arc-tangent bias-current profile. Other parameters are the same as (a), but the storage operation fails. (c) Qubit storage in larger resonator with $R = 13.7 \mu\text{m}$; the other parameters are as in (a). Storage performs poorly.

$$\begin{aligned} \dot{c}_{0n} &= \frac{g}{\hbar} \sqrt{n} \langle 0|\delta|1\rangle e^{i\omega_d t} c_{1,n-1}, \\ \dot{c}_{1n} &= -\frac{g}{\hbar} \sqrt{n+1} \langle 0|\delta|1\rangle e^{-i\omega_d t} c_{0,n+1}. \end{aligned} \quad (3)$$

At time $t = 0$ we prepare the JJ in the state $\alpha|0\rangle_J + \beta|1\rangle_J$, leaving the resonator in the ground state $|0\rangle_{\text{res}}$. We then allow the junction and resonator to interact on resonance for a time interval $\Delta t = \pi/\Omega_0$, where $\Omega_0 \equiv 2g|\langle 0|\delta|1\rangle|/\hbar$ is the vacuum Rabi frequency (for $\omega_d = 0$). We then bring the systems out of resonance and the resonator is found to be in the same pure state,

$$\alpha e^{-i\pi E_{00}/\hbar\Omega_0} |0\rangle_{\text{res}} + \beta \text{sgn}(\langle 0|\delta|1\rangle) e^{-i\pi E_{01}/\hbar\Omega_0} |1\rangle_{\text{res}},$$

apart from expected phase factors. The JJ state has actually been swapped with that of the resonator. The cavity-QED analog of this operation has been demonstrated in Ref. [15].

To assess the limitations of the RWA and examine the feasibility of future experiments, we also solve Eq. (2) numerically, including all quasibound JJ states present, and requiring convergence as a function of the resonator's Hilbert-space dimension. The simulations assume a JJ with parameters corresponding to that of Ref. [3], namely, $E_J = 43.1 \text{ meV}$ and $E_C = 53.4 \text{ neV}$, and a 10 GHz AlN resonator with $b = 0.57 \mu\text{m}$ and $R = 1.37 \mu\text{m}$ [16], as shown in Fig. 2. For this split-gate resonator, $g = 0.82 \mu\text{eV}$. We used a 4th-order Runge-Kutta method with a time step of 1 fs. Accurate s -dependent junction energies ϵ_m and eigenfunctions $\psi_m(\delta)$ were computed by diagonalizing H_J in a basis of harmonic oscillator states defined by a quadratic expansion of $U(\delta)$ about its minima, and for the range of bias currents used here found to be always well approximated by the harmonic values. Our qubit storage results are shown in Fig. 4. The initial state is $|10\rangle$, corresponding to the case $\alpha = 0$, $\beta = 1$. After 10 ns, the bias current is adiabatically changed to the

TABLE I. State amplitudes c_{mn} after phase qubit storage.

Probability amplitude	$\text{Re}c_{mn}$	$\text{Im}c_{mn}$	$ c_{mn} ^2$
c_{00}	0.010	-0.003	0.000
c_{01}	0.257	0.965	0.998
c_{10}	0.009	0.042	0.002
c_{11}	0.010	-0.003	0.000

value $s = 0.929$, bringing the qubit in resonance with $\hbar\omega_0$. The JJ is held in resonance for 35.1 ns, half a Rabi period, and then detuned. $s(t)$ has a trapezoidal shape with a crossover time of 0.5 ns. In Fig. 4(a) the storage operation is successful, and the *magnitudes* of the final probability amplitudes, recorded in Table I, are extremely close to the desired RWA values. The *phases* of the c_{mn} after storage, however, are not correctly given by the RWA unless $g/\Delta E$ is much smaller. We have verified that the nonadiabatic corrections caused by a time-varying bias do not significantly affect the results presented here; this will be discussed in a future publication.

We also find that the success of a qubit storage depends quite sensitively on the shape of the profile $s(t)$. Our simulations show that the time during which s switches should be at least exponentially localized. This can be understood by recalling that in the $Q \rightarrow \infty$ limit the RWA requires the qubit to be exactly in resonance with the resonator. Therefore one must bring the JJ into resonance as quickly as possible without violating adiabaticity. The power-law tails associated with an arc-tangent function, for example, lead to unacceptable deviations from the desired behavior, as illustrated in Fig. 4(b), even though the difference in $s(t)$ is barely visible. Furthermore, a successful storage also requires g to be considerably smaller than ΔE : In Fig. 4(a), $g/\Delta E$ is 2%, whereas the storage fails when the resonator radius R is increased to $13.7 \mu\text{m}$, as shown in Fig. 4(c), even though $g/\Delta E$ is then only about 20%.

To transfer a qubit state $|1\rangle$ between two JJs, the state is loaded into the first junction and the bias current s_1 adjusted to bring that junction into resonance with the resonator for half a Rabi period. This stores the JJ state in the resonator. After the first junction is taken out of

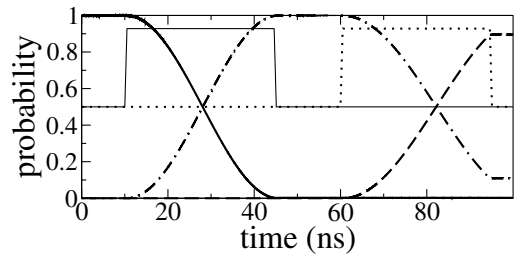


FIG. 5. Qubit transfer between two junctions. The solid curve is $|c_{100}|^2$, the dash-dotted curve is $|c_{001}|^2$, and the dashed curve is $|c_{010}|^2$. Thin, solid, and dotted curves show s_1 and s_2 , respectively.

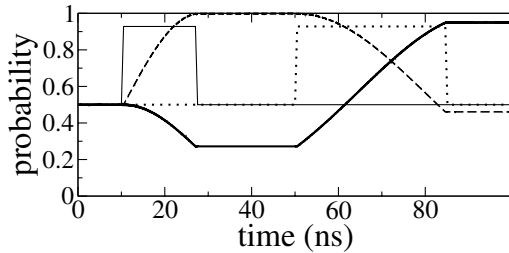


FIG. 6. JJ entanglement. The dashed curve is the probability to be in the state (in the interaction representation) $(|100\rangle + |001\rangle)/\sqrt{2}$, and the thick solid curve is for $(|100\rangle - |010\rangle)/\sqrt{2}$. Thin, solid, and dotted curves are s_1 and s_2 .

resonance, the second one is brought into resonance for half a Rabi period, passing the state to the second JJ. We have simulated this operation, assuming two identical JJs coupled to a resonator as in Fig. 2. Parameters are the same as in Fig. 4(a). Our results are shown in Fig. 5, where $c_{m_1 m_2 n}$ is the (interaction representation) probability amplitude to find the system in the state $|m_1 m_2 n\rangle$, with m_1 and m_2 labeling the states of the two JJs and n the phonon occupation number of the resonator.

Finally, we can prepare an *entangled* state of two JJs connected to a common resonator by bringing the first junction into resonance with the resonator for one-quarter of a Rabi period [17], which, according to our RWA analysis, produces the state $(|100\rangle + |001\rangle)/\sqrt{2}$. After bringing the second JJ into resonance for half a Rabi period, the state of the resonator and second JJ are swapped as $|001\rangle \rightarrow -|010\rangle$, the sign change following from (3), leaving the system in the state $(|100\rangle - |010\rangle)/\sqrt{2}$, where the resonator is in the ground state and the JJs are maximally entangled. Our simulations of this operation, the results of which are presented in Fig. 6, demonstrate successful entanglement with a fidelity of 95%. The system parameters are the same as in Fig. 5.

The quantum-information-processing operations described here require a minimum coherence time of order 100 ns, a time already demonstrated in the phase qubit [18]. More extensive operations could be performed with a coherence time of a few hundred nanoseconds, which should be achievable in the phase qubit, for which estimates fall in the 1 to 10 μs range [19]. The mechanical resonator must also achieve similar coherence times; using standard results for the coherence time of a particle coupled to a dissipative environment [20], we estimate the quantum-coherence time of an n -phonon state to be the lesser of $\tau \approx \hbar Q/k_B T(n + 1/2)$ and the energy decay lifetime Q/ω_0 . At 20 mK, the $|1\rangle$ state of our resonator is determined by the decay lifetime, which for $Q \approx 3500$ is about 300 ns.

A. N. C. and M. R. G. were supported by the Research Corporation, and M. R. G. was supported by NSF CAREER Grant No. DMR-0093217.

- [1] Y. Makhlin, G. Schön, and A. Shnirman, *Rev. Mod. Phys.* **73**, 357 (2001).
- [2] Y. Yu, S. Han, X. Chu, S.-I. Chu, and Z. Wang, *Science* **296**, 889 (2002).
- [3] J. M. Martinis, S. Nam, J. Aumentado, and C. Urbina, *Phys. Rev. Lett.* **89**, 117901 (2002).
- [4] A. J. Berkley *et al.*, *Science* **300**, 1548 (2003); F.W. Strauch *et al.*, *Phys. Rev. Lett.* **91**, 167005 (2003).
- [5] Y. Nakamura, Yu. A. Pashkin, and J.S. Tsai, *Nature (London)* **398**, 786 (1999); D. Vion *et al.*, *Science* **296**, 886 (2002); T. Yamamoto, Yu. A. Pashkin, O. Astafiev, Y. Nakamura, and J.S. Tsai, *Nature (London)* **425**, 941 (2003).
- [6] A. Shnirman, G. Schön, and Z. Hermon, *Phys. Rev. Lett.* **79**, 2371 (1997); Y. Makhlin, G. Schön, and A. Shnirman, *Nature (London)* **398**, 305 (1999); A. Blais, A. M. van den Brink, and A. M. Zagoskin, *Phys. Rev. Lett.* **90**, 127901 (2003); F. Plastina and G. Falci, *Phys. Rev. B* **67**, 224514 (2003).
- [7] O. Buisson and F.W.J. Heeking, in *Macroscopic Quantum Coherence and Quantum Computing*, edited by D.V. Averin, B. Ruggiero, and P. Silvestrini (Kluwer, New York, 2001), p. 137; F. Marquardt and C. Bruder, *Phys. Rev. B* **63**, 54514 (2001).
- [8] A. D. Armour, M. P. Blencowe, and K. C. Schwab, *Phys. Rev. Lett.* **88**, 148301 (2002).
- [9] A. Barone and G. Paterno, *Physics and Applications of the Josephson Effect* (Wiley, New York, 1982).
- [10] R. Ruby, P. Bradley, J. Larson, Y. Oshmyansky, and D. Figueredo, in *Technical Digest 2001 IEEE International Solid-State Circuits Conference Proceedings* (IEEE, Piscataway, NJ, 2001), p. 120.
- [11] X. M. H. Huang, C. A. Zorman, M. Mehregany, and M. L. Roukes, *Nature (London)* **421**, 496 (2003).
- [12] A. N. Cleland, M. Pophristic, and I. Ferguson, *Appl. Phys. Lett.* **79**, 2070 (2001).
- [13] In the $b \ll R$ limit, ω_0 is determined by the resonator thickness b , independent of the radius R , and for fixed b the interaction strength g is linearly proportional to R .
- [14] M. O. Scully and M. S. Zubairy, *Quantum Optics* (Cambridge University Press, Cambridge, 1997).
- [15] X. Maître, E. Hagley, G. Nogues, C. Wunderlich, P. Goy, M. Brune, J. M. Raimond, and S. Haroche, *Phys. Rev. Lett.* **79**, 769 (1997).
- [16] AlN has a density $\rho = 3.26 \text{ g/cm}^3$, piezoelectric modulus $e_{33} = 1.46 \text{ C/m}^2$, dielectric constant $\epsilon_{33} = 10.7\epsilon_0$, and elastic stiffness $c_{33} = 395 \text{ GPa}$.
- [17] E. Hagley, X. Maître, G. Nogues, C. Wunderlich, M. Brune, J. M. Raimond, and S. Haroche, *Phys. Rev. Lett.* **79**, 1 (1997).
- [18] J. M. Martinis (private communication).
- [19] J. M. Martinis, S. Nam, J. Aumentado, and K. M. Lang, *Phys. Rev. B* **67**, 94510 (2003).
- [20] E. Joos, in *Decoherence and the Appearance of a Classical World in Quantum Theory*, edited by D. Giulini *et al.* (Springer-Verlag, Berlin, 1996), p. 35.